



## A study of the effects of mixtures of solvents on CO<sub>2</sub>/N<sub>2</sub> gas separation in polysulfone flat sheet membranes

Ali A. Abdulabbas<sup>1,\*</sup>, Thamer J. Mohammed<sup>2</sup> and Tahseen A. Al-Hattab<sup>3</sup>

<sup>1</sup>Department of Chemical engineering and Petroleum Industries, Al-Amarah University College, Maysan, Iraq

<sup>2</sup>Chemical engineering Department, University of Technology-Iraq, Baghdad, Iraq

<sup>3</sup>Chemical engineering Department, College of Engineering, University of Babylon, Iraq

### Article information

#### Article history:

Received: January, 11, 2023

Accepted: March, 19, 2023

Available online: April, 08, 2023

#### Keywords:

Carbon capture,  
Polysulfone (PSF),  
CO<sub>2</sub>/N<sub>2</sub> separation,  
A volatile solvent

#### \*Corresponding Author:

Ali A. Abdulabbas

[che.20.02@grad.uotechnology.edu.iq](mailto:che.20.02@grad.uotechnology.edu.iq)

### Abstract

Different solvents were used to produce polysulfone (PSF) membranes. These solvents included, Tetrahydrofuran (THF), N,N-dimethylacetamide(DMAc), Dichloromethane(DCM) and N-methyl-2-pyrrolidone (NMP).

Gas permeability was greatest for the PSF membrane prepared with NMP, while selectivity was best for the THF membrane. Tetrahydrofuran (THF) was added into the casting solution at varying loadings (from 0% to 35%) to create asymmetric membranes with excellent gas separation performance. In SEM, the layer of the membrane that was prepared with NMP as the solvent is the thickest, while the layer of the membrane that was made with NMP/THF as solvent mixture is the thinnest. In gas permeability tests, as the amount of THF increases with NMP, it has the highest CO<sub>2</sub>/N<sub>2</sub> selectivity and the lowest permeability.

PSF/NMP has the highest permeabilities for CO<sub>2</sub> (0.0728 GPU) and N<sub>2</sub>(0.0186 GPU), and the lowest selectivity for CO<sub>2</sub>/N<sub>2</sub>. Because of the thinner skin layer, CO<sub>2</sub> and N<sub>2</sub> are able to pass through more easily, while the low selectivity is the result of a surface defect in the form of a pin-hole. The maximum CO<sub>2</sub>/N<sub>2</sub> selectivity is 8.69 for PSF/ NMP/THF.

DOI: <http://doi.org/10.55699/ijogr.2023.0301.1035>, Oil and Gas Engineering Department, University of Technology-Iraq

This is an open access article under the CC BY 4.0 license <http://creativecommons.org/licenses/by/4.0>

## 1. Introduction

Global warming induced by CO<sub>2</sub> emissions into the atmosphere as well as the generation of clean and conventional energy has heightened awareness of the requirement for CO<sub>2</sub> capture[1]. There are many ways to separate and purify gases. Some of these ways are adsorption, absorption, cryogenic, and membrane separation[2]. Today, reduced capital costs, clean energy, and easy processing have established membrane technology as a cost-effective membrane separation process[3]. Membrane-based gas separation uses differential permeability to separate components from mixtures[4]. It has expanded due to new materials and technologies. Therefore, they are used to separate CO<sub>2</sub> from flue gas and natural gas, and remove organic pollutants from industrial effluents[5].

A polymeric membrane's permeability and selectivity were mainly controlled by its physical and chemical structure[6]. In addition, the molecular size, boiling point, and interactions with polymer chains that are employed to construct polymer-based membranes all have a significant impact on the membranes' separation performance and structure. When the solubility factor of the solvent is close to that of the polymer, the solvent is strongly attracted to the polymer, causing the polymer chains to stretch[7]. Due to the decrease in intermolecular free volumes, membrane selectivity is improved[8].

Evaporation of solvents with larger molecular weights leaves behind more void space in the polymeric material, facilitating gas transport, so evaporation rates are proportional to the solvent's boiling point. Since the molecules' velocity and free volume both increase when the solvent evaporates out of the structure, permeability also increases[9]. Furthermore, the separation properties of membranes may be affected by the characteristics of the solvents used in their preparation. So, selecting the appropriate solvent or mixture of solvents is essential for producing a membrane with desirable separation performance[10].

Polyethersulfone (PES), polysulfone (PSF), and polyimide are among the most widely utilized gas separation polymeric materials[11]. PSF membranes were chosen for their commercial availability, treatment simplicity, and higher separation[12]. It is soluble in a variety of nonvolatile solvents, including N-methyl pyrrolidinone (NMP) and N-dimethylacetamide (DMAc), but less so in volatile solvents such as tetrahydrofuran (THF) and dichloromethane (DCM). As a result, it is widely used in the fabrication of asymmetric membranes for a wide range of commercial uses. Mazinani et al.[13] used four solvents (NMP, DMF, DMAc, and DMSO) at 25 °C to study liquid–liquid demixing and morphologies. DMAc and water instantaneously demixed, forming finger-like macrovoids, while DMSO has a reduced diffusion rate and suppresses solvent exchange, creating a sponge structure.

Alaei et al.[14] studied polyethersulfone (PES) in a variety of solvents. They found that DMAc had more porosity and permeance than other solvents due to the different solubility values of the solvents. Furthermore, the molar ratio of various solvents can have an impact on membrane structures. Mousavi and Zadhoush[15] analyzed the effects of solvent combinations on membrane designs and characteristics. When the concentration of 2-pyrrolidone was increased to 75%, the morphology changed to finger macrovoids. In addition, solvent choice affects asymmetric membrane morphology and separation efficiency. N-methyl-2-pyrrolidone (NMP) is the most utilized water-soluble solvent because of its high solubility for PSF, low toxicity, and water solubility. A co-solvent is often a volatile solvent as tetrahydrofuran (THF)[16].

In this work, the performance of CO<sub>2</sub>/N<sub>2</sub> separation in polysulfone (PSF) membranes is investigated with pure (NMP, DMAc, DCM and THF) and mixed solvents, such as NMP and tetrahydrofuran (THF) with varied concentrations. Therefore, the CO<sub>2</sub>/N<sub>2</sub> separation and chemical stability of membranes, as well as their morphology, were evaluated.

## 2. Experimental

### 2.1 Materials

Polysulfone (PSF) ( $M_w = 80,000$  g/mol, density  $1.24$  g/cm<sup>3</sup>,  $T_g = 187$  C) was provided from (Germany). Sigma Aldrich supplied the solvents, which included (NMP), (DMAc), (DCM) and (THF). It was chosen to use the distilled water for membrane precipitation as a coagulation medium. Table 1 presents the characteristics of all membranes.

**Table 1 Chemical components and their characteristics[17,18]**

Name	Molecular formula	Molar mass(g/mol)	Density(g/cm <sup>3</sup> )	Boiling point(°C)
<i>NMP</i>	C <sub>5</sub> H <sub>9</sub> NO	99.13	1.028	203
<i>THF</i>	C <sub>4</sub> H <sub>8</sub> O	72.11	0.889	66
<i>DMAc</i>	C <sub>4</sub> H <sub>9</sub> NO	87.12	0.94	166
<i>DCM</i>	CH <sub>2</sub> Cl <sub>2</sub>	84.93	1.324	40
<i>Water</i>	H <sub>2</sub> O	18.02	1.000	100

**Table 2 preparation ratios for the membrane**

Membrane	Polymer concentration [%wt]	Solvent[%wt]			
		NMP	THF	DMAc	DCM
<i>PSF-1</i>	30	70	0	0	0
<i>PSF-2</i>	30	57.75	12.25	0	0
<i>PSF-3</i>	30	45.5	24.5	0	0
<i>PSF-4</i>	30	0	70	0	0
<i>PSF-5</i>	30	0	0	70	0
<i>PSF-6</i>	30	0	0	0	70

### 2.2 Synthesis of PSF membranes

By dissolving polysulfone in the various solvent combinations outlined in Table 2, five distinct PSF flat sheet membranes were produced. Polysulfone flat sheet membranes were produced using the phase inversion procedure and immersion precipitation technique (Figure 1). In order to obtain a homogeneous solution, the polymer is dissolved in a solvent, and the solution is stirred with a magnetic stirrer at 250 rpm at 55 °C for 9 hours. The uniform solution was then cast onto a glass plate with a thickness of 0.2 mm and remained for 20 seconds. Additionally, the casting was soaked in a coagulation bath of distilled water at 25 °C for 12 hours. The membrane was left out in the atmosphere for 48 hours to dry completely.

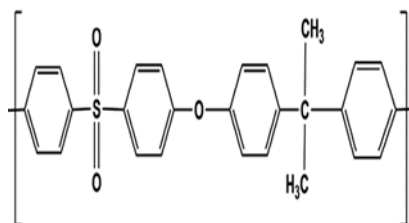


**Figure 1 Schematic depiction of the polysulfone structure[19].**

## 2.3 Characterization of the PSF membrane

### 2.3.1 Structure and morphology using FESEM

Field emission scanning electron microscopy (FESEM) was used to study the surface morphologies of asymmetric PSF membranes by Inspect F50 (ELECMI, Spain). It was able to obtain an image of the structure of the skin as well as a cross-section of membranes that had been presented using various composition.

### 2.3.2 FTIR functional group classification

FTIR spectroscopy was used to determine the types of functional groups found in asymmetric PSF membranes. For these experiments, the IRTRANCE-100 was used alongside a single-reflection ATR attachment to scan the samples. Cutting the materials into smaller pieces allowed for easier scanning at wavelengths ranging from  $400\text{ cm}^{-1}$  to  $4000\text{ cm}^{-1}$ .

## 2.4 Gas Permeation experiments

Gas permeation tests were performed with a constant pressure/variable volume setup using the  $\text{CO}_2$ , and  $\text{N}_2$ . The setup applied included circular membrane discs with an effective permeation area of  $12.5\text{ cm}^2$  as shown in Fig 2. The rate of penetration in the constant pressure system was determined from the rate of the rise in volume ( $dv/dt$ ) using. The following equation can be used to calculate the known permeate side[20]:

$$P_i/t = Q_i/A\Delta p \quad (1)$$

Where  $P_i/t$  is permeance of gas  $i$  expressed in GPU, with 1 GPU equating to  $10^{-6}\text{ cm}^3\text{ (STP) cm}^{-2}\text{ s}^{-1}\text{ cmHg}^{-1}$ ,  $Q_i$  is the gas permeation rate,  $\Delta p$  is the pressure differential across the membrane,  $A$  is the effective area, and  $t$  is the thickness of the membrane. The membrane's theoretical selectivity was calculated using the following formula[21]:

$$\alpha_{ij} = \left( \frac{P_i}{P_j} \right) = (P_i/t)/(P_j/t) \quad (2)$$

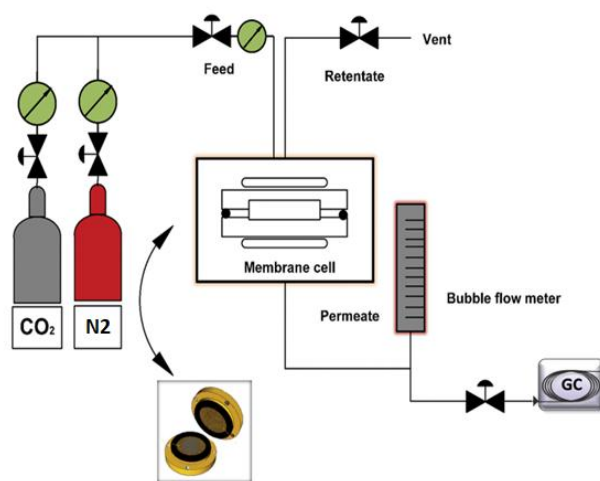


Figure 2 Gas permeance system of  $\text{CO}_2$  and  $\text{N}_2$ .

### 3 . Result and discussion

#### 3.1 Effects of solvent on the PSF membrane

Different casting solutions, including NMP, DMAc, THF, and DCM, were used to produce polysulfone membranes because of their varying solubilities and boiling points (Table 3). The PSF membrane's gas performance at 1 bars and 25°C was measured to evaluate its effect. The results showed that solubility of the polymer/solvent plays an essential role in the membrane's gas permeability. Also, the results confirm that molecule size and boiling point have an impact on the separation properties and structure of PSF membranes. The permeability characteristics of PSF membranes produced with various solvents decreases with increasing penetrant size ( $N_2 > CO_2$ ). PSF-THF has the lowest permeability, while PSF-NMP has the highest permeability of the samples. In contrast,  $CO_2/N_2$  selectivities move in a different direction depending on the solvents. Therefore, molecular size and the boiling temperature of the solvent can affect the fabricated PSF membranes, as observed in Table 4[18]. Because the PSF membrane produced using NMP and THF had the best permeability and selectivity, the influence of the solvent in solution is discussed in the next section. Also, the morphology and performance are examined for PSF membranes prepared with pure NMP and a mixture of NMP and THF.

**Table 3 Solvent and polysulfone Hansen solubility parameters[23,24]**

Material	$\delta_D$	$\delta_p$	$\delta_h$	$\delta_t$	$ \delta_t, PSF - \delta_t, Solvent $
<i>PSF</i>	19.7	8.3	8.3	22.93	-
<i>NMP</i>	18	12.3	7.2	22.96	0.03
<i>DMAc</i>	16.8	11.5	10.2	22.77	0.16
<i>THF</i>	16.8	5.7	8	19.46	3.47
<i>DCM</i>	18.2	6.3	6.1	20.20	2.73
<i>Water</i>	15.5	16	42.3	47.81	-

$\delta_d$ ,  $\delta_h$  and  $\delta_p$  represented the dispersion force solubility, hydrogen bonding solubility, and polar solubility factors, respectively, while,  $\delta_t$  was the total solubility factor, which is determined by the following equation:

$$\delta_t = \sqrt{\delta_d^2 + \delta_p^2 + \delta_h^2} \quad (3)$$

**Table 4 Permeation of the membranes with different solvents at 1 bar and 25 C**

Membrane	Permeability (GPU)		Selectivity $CO_2/N_2$
	$CO_2$	$N_2$	
<i>PSF-NMP</i>	0.0662	0.0105	6.25
<i>PSF-THF</i>	0.0448	0.0058	7.72
<i>PSF-DMAc</i>	0.052	0.0081	6.41
<i>PSF-DMC</i>	0.062	0.016	3.87

#### 3.2 Effects of solvent on membrane morphology

The effect of each solvent on the morphologies of the generated asymmetric PSF flat sheet membrane was evaluated using FESEM. It was found that PSF membranes fabricated with varied THF compositions had a large of structural characteristics and thicknesses. The evaporation stage, including the evaporation period prior to immersion in the coagulation bath, affects the membrane thickness in addition to the membrane formation itself [24]. Since the membrane gets thicker or thinner when it comes in contact with air, the evaporation step can affect how well the separation works [25]. As a result, using either a

volatile solvent (THF) or a less volatile solvent(NMP) will alter the evaporation rate of the solvent and the thickness of the skin in the casting solution[26].

The skin thickness of membranes cast from dope made using an NMP/THF mixture rather than pure NMP is greater. Thus, the membrane thickness of PSF-1, PSF-2, and PSF-3 to be 116  $\mu\text{m}$ , 131  $\mu\text{m}$ , and 184  $\mu\text{m}$ , respectively. PSF-3 has the thickest skin of the three due to a high THF content. In membranes fabricated with solvent variation, a significant difference in structure was obtained. Also adding THF to the casting solution, can be prevent macro-voids from forming during instantaneous demixing and change the appearance of the membrane from macro-voids to structures that appear as sponges[27]. The PSF-3 membrane has a higher porosity than PSF-2 and PSF-1 membranes[28]. The surface top of membranes are shown in Figure 3 (d,e,f). It has a surface layer with a variety of pinholes of various sizes, while PSF-3 membrane has a smooth surface with a greater number of small pinholes. But both PSF-1 and PSF-2 have fewer and larger pinholes than PSF-3. This explains the effect of solvent variability and evaporation rate on membrane casting, resulting in a skin layer with different number and size of pores[29]. From Figure 4, compared to PSF-1, the dense layer in PSF-2 and PSF-3 has a greater thickness and a more extensive porous structure. This confirms that the substructure of the membrane generated from NMP/THF required a high time for demixing when the casting layer of membrane was immersed in a water bath, indicating a lower coagulation value[30]. Figure 4(a) shows a symmetric membrane with an interconnected system of small pores produced by pure NMP solvent. This explains that the use of non-volatile NMP reduces solvent evaporation, which is necessary for the fabrication of an asymmetric layer. As shown in Fig.4(b, c) for the membranes prepared with a solvent mixture of THF and NMP, rapid mixing takes place only if the solvent and the non-solvent have a strong affinity for each other[31]. THF has a lesser affinity and miscibility with water than NMP. Therefore, THF and water have delayed demixing, but NMP and water have rapid demixing[17].

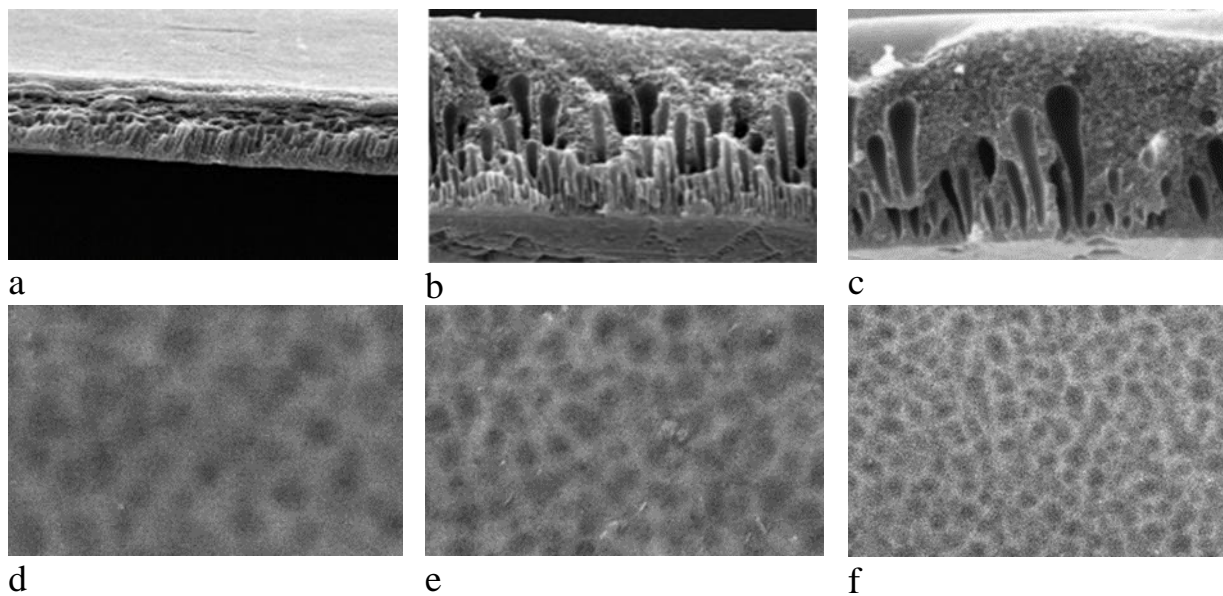


**Figure 3** FESEM images of cross-sections and top surface of PSF membranes

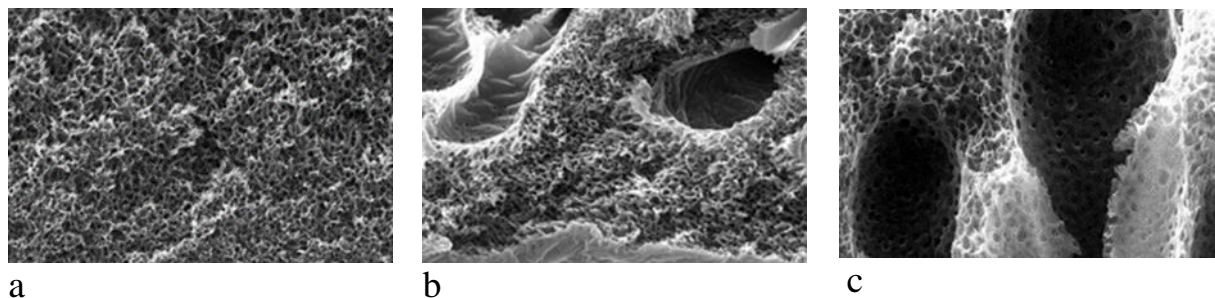
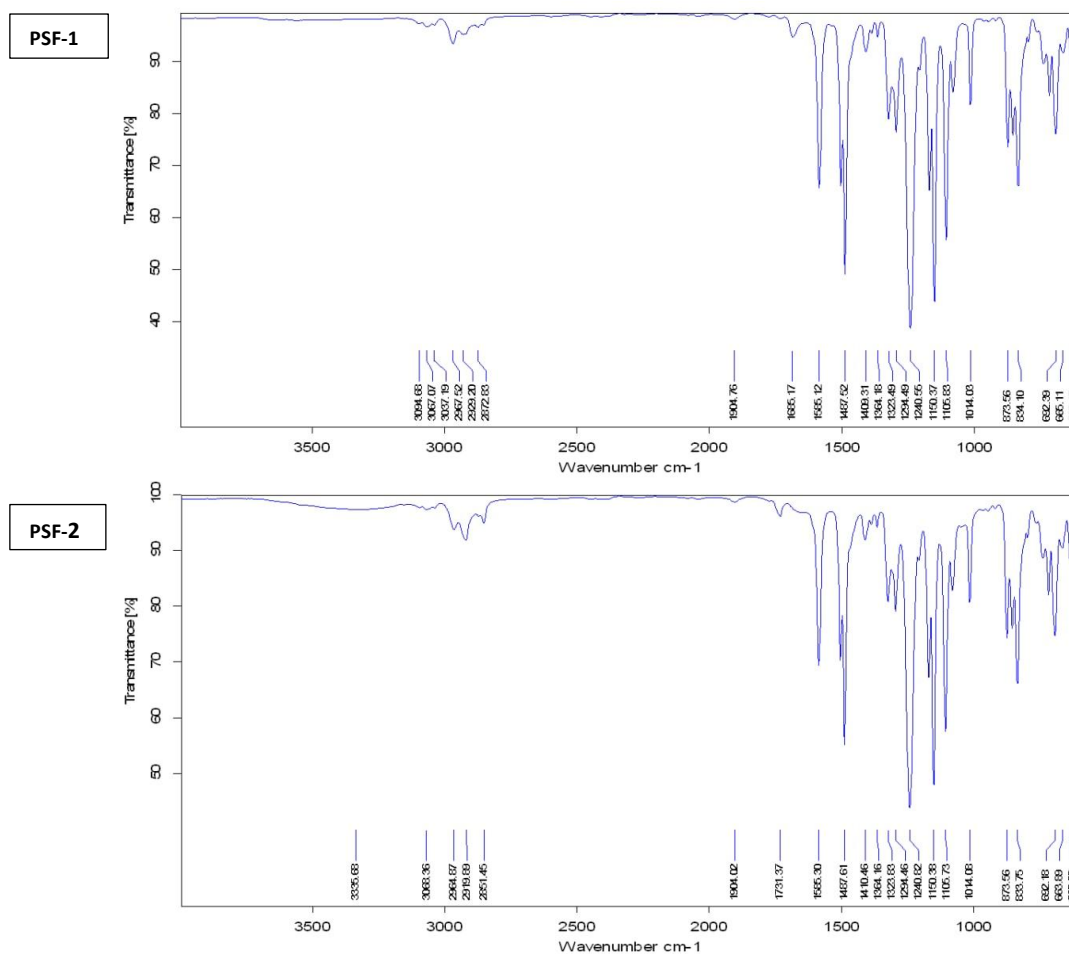


Figure 4 The cross-section of Asymmetric PSF membrane

### 3.3 Chemical membrane analysis

Small differences in wavelength and transmittance percentage were observed across polymer concentrations of PSF-1, PSF-2, and PSF-3 membranes are chosen, and changes in the functional graph, wavelength, and transmittance percentage were measured. Figure 5 and Table 5 display the infrared spectral differences between membranes. As the amounts of polymer and solvent changed, the polymer and solvent interacted and bonded in different ways. This caused the wavelength of the functional group to change. Polysulfone molecules may have interacted with the solvent on a molecular scale, resulting in this effect.



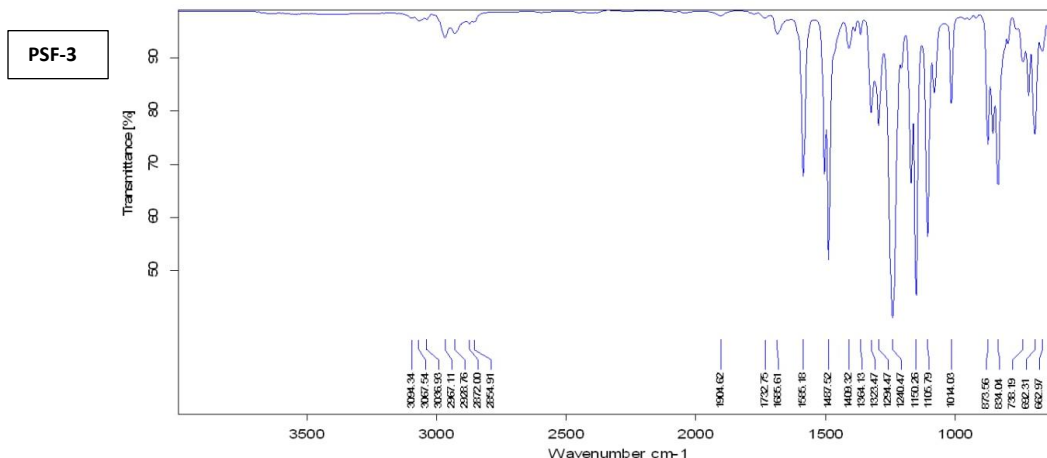


Figure 5 Chemical analysis of PSF-1, PSF-2 and PSF-3 Membranes

Table 5 IR spectra of polymers dissolved in a variety of solvents at 30% concentration

Name group	PSF-1	PSF-2	PSF-3
<i>diaryl sulfone (R-SO<sub>2</sub>-R)</i>	1150.37	1150.38	1150.26
<i>diaryl ether (C-O-C)</i>	1240.56	1240.82	1240.82
<i>Aromatic C=C</i>	1485	1485	1485
<i>Aliphatic C-H</i>	2872.83	2851.45	2872
<i>Aliphatic C-H scissoring and bending</i>	1409.31	1410.46	1409.32
<i>Phenyl ring substitution band</i>	692.39	692.18	692.31

### 3.4 The efficiency of gas separation

In the gas permeation system, the separation capabilities of the membrane were evaluated. At an input gas pressure of 2 bars and a temperature of 35 °C, the ability of CO<sub>2</sub> and N<sub>2</sub> to pass through three membranes (PSF-1, PSF-2, and PSF-3) was measured. According to Table 6, there is a noticeable variation in the difference when CO<sub>2</sub> and N<sub>2</sub> are separated. PSF-1 has the highest permeabilities for CO<sub>2</sub> (0.0728 GPU) and N<sub>2</sub>(0.0186 GPU), and the lowest selectivity for CO<sub>2</sub>/N<sub>2</sub>. Because of the thinner skin layer, CO<sub>2</sub> and N<sub>2</sub> are able to pass through more easily, while the low selectivity is the result of a surface defect in the form of a pin-hole. The maximum CO<sub>2</sub>/N<sub>2</sub> selectivity is 8.69 for PSF-3.

Table 6 Permeability and selectivity values of CO<sub>2</sub>/N<sub>2</sub> for the PSF membrane (2 bars, 35C)

Membrane	Permeance (GPU)		Selectivity
	CO <sub>2</sub>	N <sub>2</sub>	
PSF-1	0.0728	0.0186	3.91
PSF-2	0.0369	0.00576	6.40
PSF-3	0.0226	0.00261	8.69

CO<sub>2</sub> and N<sub>2</sub> have the lowest permeability of the three membranes. Thus, the use of THF as a solvent improved the selectivity of asymmetric PSF, which is mostly attributable to a comparatively defect-free surface layer. With CO<sub>2</sub>/N<sub>2</sub> selectivity of 6.4, PSF-2 produces average results. CO<sub>2</sub> has a permeability that is between PSF-1 and PSF-3, but N<sub>2</sub> has a permeability that is more than PSF-3. In general, by increasing the amount of volatile solvent in the polymer concentration, the membrane becomes more selective and less permeable.



#### 4. Conclusions

In the current study, NMP, THF, DMAc, and DCM were used as casting solvents to study the PSF membrane's gas permeation characteristics at 25 °C and 1 bar. In comparison to other polymer-solvent combinations, PSF/NMP has greater permeability because of its lower solubility factor compared with PSF, highest boiling point, and molecular volume. PSF/THF has high selectivity due to its low boiling point, and small molecular size, so it is used in casting solutions in combination with NMP. The polymer concentration is maintained in the casting solution; three different composition solvents were chosen. Scanning Electron Microscopy (SEM) is applied to analyze membrane morphology. The results revealed that various casting solutions produced various types of membrane cross-sections and membrane surfaces. The chemical structure's processes were studied using Fourier Transform Infrared Spectroscopy (FTIR). It appeared that the functional group's chemical structure took on a different molecular form in each solvent, indicating a trend.

#### Reference

- [1] A. Fakhar, M. Sadeghi, M. Dinari, M. Zarabadipoor, and R. Lammertink, "Elucidating the effect of chain extenders substituted by aliphatic side chains on morphology and gas separation of polyurethanes," *Eur. Polym. J.*, vol. 122, no. August 2019, p. 109346, 2020.
- [2] H. Waheed and A. Hussain, "Effect of Polyvinyl Pyrrolidone on Morphology and Performance of Cellulose Acetate Based Dialysis Membrane," *Eng. Technol. Appl. Sci. Res.*, vol. 9, no. 1, pp. 3744–3749, 2019.
- [3] A. V. Mahenthiran and Z. A. Jawad, "A prospective concept on the fabrication of blend pes/peg/dmf/nmp mixed matrix membranes with functionalised carbon nanotubes for co2/n2 separation," *Membranes (Basel)*, vol. 11, no. 7, 2021.
- [4] M. Vinoba, M. Bhagiyalakshmi, Y. Alqaheem, A. A. Alomair, A. Pérez, and M. S. Rana, "Recent progress of fillers in mixed matrix membranes for CO2 separation: A review," *Sep. Purif. Technol.*, vol. 188, pp. 431–450, 2017.
- [5] "SPE Polymers - 2020 - Fakhar - Gas separation through polyurethane ZnO mixed matrix membranes and mathematical modeling of.pdf."
- [6] S. Li, Y. Liu, D. Wong, and J. Yang, "Recent advances in polymer-inorganic mixed matrix membranes for co2 separation," *Polymers (Basel)*, vol. 13, no. 15, 2021.
- [7] Z. Li, J. Ren, A. G. Fane, D. F. Li, and F. S. Wong, "Influence of solvent on the structure and performance of cellulose acetate membranes," *Journal of Membrane Science*, vol. 279, no. 1–2, pp. 601–607, 2006.
- [8] Y. J. Fu, C. C. Hu, H. zhi Qui, K. R. Lee, and J. Y. Lai, "Effects of residual solvent on gas separation properties of polyimide membranes," *Separation and Purification Technology*, vol. 62, no. 1, pp. 175–182, 2008.
- [9] J. Ahmad and M. B. Hägg, "Development of matrimid/zeolite 4A mixed matrix membranes using low boiling point solvent," *Separation and Purification Technology*, vol. 115, pp. 190–197, 2013.
- [10] L. Shao, T. S. Chung, G. Wensley, S. H. Goh, and K. P. Pramoda, "Casting solvent effects on morphologies, gas transport properties of a novel 6FDA/PMDA-TMMDA copolyimide membrane and its derived carbon membranes," *Journal of Membrane Science*, vol. 244, no. 1–2, pp. 77–87, 2004.
- [11] A. Mukhtar *et al.*, "CO2 capturing, thermo-kinetic principles, synthesis and amine functionalization of covalent organic polymers for CO2 separation from natural gas: A review," *J. Nat. Gas Sci. Eng.*, vol. 77, no. January, p. 103203, 2020.
- [12] A. A. Abdulabbas and T. J. Mohammed, "Preparation of Mixed Matrix Membranes containing COF materials for CO 2 removal from Natural Gas / Review," 1991.
- [13] J. Ding, J. Zeng, Y. Zeng, Z. Yuan, X. Huang, and Y. Wu, "Engineering multistructure poly(vinylidene fluoride) membranes modified by polydopamine to achieve superhydrophilicity,

- excellent permeability, and antifouling properties,” *Asia-Pacific Journal of Chemical Engineering*, vol. 16, no. 2, 2021.
- [14] S. Alibakhshi, M. Youssefi, S. S. Hosseini, and A. Zadhoush, “Tuning morphology and transport in ultrafiltration membranes derived from polyethersulfone through exploration of dope formulation and characteristics,” *Mater. Res. Express*, vol. 6, no. 12, 2019.
- [15] X. Dong, A. Al-Jumaily, and I. C. Escobar, “Investigation of the use of a bio-derived solvent for non-solvent-induced phase separation (NIPS) fabrication of polysulfone membranes,” *Membranes (Basel)*, vol. 8, no. 2, 2018.
- [16] X. Dong, D. Lu, T. A. L. Harris, and I. C. Escobar, “Polymers and solvents used in membrane fabrication: A review focusing on sustainable membrane development,” *Membranes (Basel)*, vol. 11, no. 5, 2021.
- [17] M. A. U. R. Alvi *et al.*, “Polymer concentration and solvent variation correlation with the morphology and water filtration analysis of polyether sulfone microfiltration membrane,” *Adv. Polym. Technol.*, vol. 2019, 2019.
- [18] R. M. Almuhtaseb, A. Awadallah-F, S. A. Al-Muhtaseb, and M. Khraisheh, “Influence of casting solvents on CO<sub>2</sub>/CH<sub>4</sub> separation using polysulfone membranes,” *Membranes (Basel)*, vol. 11, no. 4, 2021.
- [19] M. Sarfraz, A. Arshad, and M. Ba-Shammakh, “Predicting Gas Permeability through Mixed-matrix Membranes Filled with Nanofillers of Different Shapes,” *Arab. J. Sci. Eng.*, no. July, 2021.
- [20] “BookChapter-CarbonCaptureviaMixed-MatrixMembranesContainingNanomaterialsandMetal-OrganicFrameworks.pdf.”
- [21] Z. Zhang, S. Rao, Y. Han, R. Pang, and W. S. W. Ho, “CO<sub>2</sub>-selective membranes containing amino acid salts for CO<sub>2</sub>/N<sub>2</sub> separation,” *Journal of Membrane Science*, vol. 638, 2021.
- [22] S. M. Mousavi and A. Zadhoush, *Investigation of the relation between viscoelastic properties of polysulfone solutions, phase inversion process and membrane morphology: The effect of solvent power*, vol. 532. Elsevier B.V., 2017.
- [23] Z. A. Jawad, A. L. Ahmad, S. C. Low, T. L. Chew, and S. H. S. Zein, “Influence of solvent exchange time on mixed matrix membrane separation performance for CO<sub>2</sub>/N<sub>2</sub> and a kinetic sorption study,” *J. Memb. Sci.*, vol. 476, pp. 590–601, 2015.
- [24] I. U. Khan *et al.*, “ZIF-8 based polysulfone hollow fiber membranes for natural gas purification,” *Polym. Test.*, vol. 84, no. February, p. 106415, 2020.
- [25] T. Barzegar and S. Hassanajili, “Fabrication and characterization of dual layer PEBAX-SiO<sub>2</sub>/polyethersulfone nanocomposite membranes for separation of CO<sub>2</sub>/CH<sub>4</sub> gases,” *J. Appl. Polym. Sci.*, vol. 139, no. 6, pp. 1–18, 2022.
- [26] Q. Wu *et al.*, “Effect of volatile solvent and evaporation time on formation and performance of PVC/PVC-G-PEGMA blended membranes,” *RSC Advances*, vol. 9, no. 59, pp. 34486–34495, 2019.
- [27] R. THÜR Supervisor, I. F. J Vankelecom, and K. Leuven, “Co<sub>2</sub>-Selective Polymer and Mixed-Matrix Membranes for CO<sub>2</sub>/N<sub>2</sub> and CO<sub>2</sub>/CH<sub>4</sub> Separations,” no. November, 2020.
- [28] Y. Liu *et al.*, “Multifunctional covalent organic framework (COF)-Based mixed matrix membranes for enhanced CO<sub>2</sub> separation,” *J. Memb. Sci.*, vol. 618, no. July 2020, p. 118693, 2021.
- [29] F. A. H. Juber, Z. A. Jawad, B. L. F. Chin, S. P. Yeap, and T. L. Chew, “The prospect of synthesis of PES/PEG blend membranes using blend NMP/DMF for CO<sub>2</sub>/N<sub>2</sub> separation,” *J. Polym. Res.*, vol. 28, no. 5, 2021.
- [30] E. J. Vriezckolk, K. Nijmeijer, and W. M. de Vos, “Dry-wet phase inversion block copolymer membranes with a minimum evaporation step from NMP/THF mixtures,” *Journal of Membrane Science*, vol. 504, pp. 230–239, 2016.
- [31] J. You, Y. Zhao, L. Wang, and W. Bao, “Recent developments in the photocatalytic applications of covalent organic frameworks: A review,” *J. Clean. Prod.*, vol. 291, p. 125822, 2021.